# CHAPTER 6

## *Effects of morphine and alcohol on functional brain connectivity during 'resting state': a placebo-controlled crossover study in healthy young men*

*Hum Brain Mapp. 2012, 33(5), 1003-1018*

N. Khalili-Mahani, R.W.M. Zoethout, C.F. Beckmann, E. Baerends,
M.L. de Kam, R.P. Soeter, A. Dahan, M.A. van Buchem,
J.M.A. van Gerven, S.A.R.B. Rombouts

## ABSTRACT

A major challenge in central nervous system (CNS) drug research is to develop a generally applicable methodology for repeated measurements of drug effects on the entire CNS, without task-related interactions and *a priori* models. For this reason, data-driven resting-state fMRI methods are promising for pharmacological research. We aimed to investigate whether different psychoactive substances cause drug-specific effects in functional brain connectivity during resting-state. In this double blind placebo-controlled (double dummy) crossover study, seven resting-state fMRI scans were obtained in 12 healthy young men in three different drug sessions (placebo, morphine and alcohol; randomized). Drugs were administered intravenously based on validated pharmacokinetic protocols to minimize the inter- and intra-subject variance in plasma drug concentrations. Dual-regression was used to estimate whole-brain resting-state connectivity in relation to eight well-characterized resting-state networks, for each data set. A mixed effects analysis of drug by time interactions revealed dissociable changes in both pharmacodynamics and functional connectivity resulting from alcohol and morphine. Post hoc analysis of regions of interest revealed adaptive network interactions in relation to pharmacokinetic and pharmacodynamic curves. Our results illustrate the applicability of resting-state functional brain connectivity in CNS drug research.


## INTRODUCTION

One of the major challenges of central nervous system (CNS) drug discovery is to develop a generally applicable methodology to demonstrate the effects of a compound on the brain across the different phases of drug development. An optimal methodology should be minimally invasive, repeatable and able to identify overlapping and distinguishable effects of different CNS drugs with little reliance on *a priori* models for drug effects.

The advances in functional neuroimaging, especially positron emission tomography (PET) and functional magnetic resonance imaging (fMRI), have opened important frontiers for CNS drug research. However, radiation dose restrictions in PET prevent repeated intra-subject measurements within short periods of time. This is a major limitation of PET because repeated measurements allow testing different drug compounds on the same individual and minimize the within-subject variances. More importantly, repeated neuroimaging acquisitions would allow the assessment of pharmacokinetic/pharmacodynamic (PK/PD) relationships, which form the scientific basis of modern drug development.

Compared to PET, blood-oxygen-level-dependent (BOLD) fMRI is non invasive, and benefits from high temporal and spatial resolution. Until recently, fMRI was applicable in task-related designs, where pharmachologically induced changes in regional BOLD signal in response to a hypothesized CNS function (e.g. pain alleviation) were investigated. For examples see (Honey and Bullmore, 2004). One of the major limitations of this approach was the difficulty in controlling for inter-subject variations in stimulus perception or performance in task-related experiments. In addition, fMRI tasks had to be chosen to activate regions of interest based on *a priori* hypotheses about the site of drug effect (Breiter *et al.*, 1997); or about the PK/PD profile (Stein *et al.*, 1998) – which in many cases are unknown.

A recent breakthrough in neuroimaging has resulted from discovering the complex (but consistent and reliable) functional architecture of brain activity from the BOLD fluctuations (Biswal *et al.*, 2010; Bullmore and Sporns, 2009; Smith *et al.*, 2009). Today, a growing body of evidence suggests that the 'resting-state' brain activity (i.e. spontaneous BOLD fluctuations in the absence of any specific stimuli) forms spatially correlated topographies, which represent functional connections that relate to, or even predict, emotional and cognitive behavioral outcomes (Fox *et al.*, 2007; Seeley *et al.* 2007) or clinical conditions (Greicius, 2008). These resting-state networks (RSNs) represent distinct functional systems (e.g. motor, vision, attention, etc), that are reliable and reproducible (Beckmann *et al.* 2005; Biswal *et al.*, 2010; Damoiseaux *et al.*, 2006; Zuo *et al.*, 2009). Hence, if different drugs produce specific and detectable changes in the functional topography of these networks, then RSNs may become a biomarker for CNS drug research.

In this study we investigate whether *different psychoactive drug compounds (alcohol and morphine) elicit distinguishable changes in functional topography of the resting-state brain networks*. The RSN connectivity is determined in terms of similarity of temporal fluctuations in the whole brain in relation to eight networks of interest (NOI). These NOIs represent the most reliably and reproducibly detectable RSNs of functional significance (e.g. visual, somatosensory, motor, attention, working memory) (Beckmann *et al.*, 2005; Damoiseaux *et al.*, 2006). Drugs are administered under PK-controlled infusion protocols. Seven resting-state fMRIs (RS-fMRI) and several PK and PD assessments are made at controlled intervals (figure 1). We report drug-specific changes in the profile of RSN connectivity, and show their temporal relation to the profiles of drug concentrations and pharmacodynamic effects in areas where effects of morphine and alcohol are expected.

# METHODS

## *Experimental Design*

A schematic diagram of the study design and the analyses is provided in figure 1. This study is randomized, double blind (i.e. both examiner and the participant are unaware of which drugs are given), and double dummy placebo-controlled (i.e. placebo was used for each treatment, consisting of infusion of the vehicle for treatment A in parallel to the administration of active treatment B or vice versa, and two vehicle infusions in the placebo session). Alcohol and morphine are two of the most commonly used substances in addiction and pain studies with similar analgesic and euphoric effects but they also result in different autonomic responses. In humans, alcohol exerts a wide range of psychoactive effects by interacting with GABAergic, dopaminergic, serotonergic and even opiate neurotransmitter systems (Koob *et al.*, 1998). In contrast, morphine targets specific receptors (μ-opioid), which in turn interact with many other neurotransmitter systems (Contet *et al.*, 2004). This within-subject design aimed to test whether drug-specific effects on the RSN connectivity would be detectable and whether their profile corresponded to the PK and PD profiles we measured. However, both alcohol and morphine have dose-dependent effects on the regional cerebral blood flow (Blaha *et al.*, 2003; Wagner *et al.*, 2001), and pharmacodynamic effects can significantly vary across individuals. Hence, we applied previously validated infusion regimens to achieve approximately steady state serum levels and controlled pharmacodynamic effects. The infusion protocols were based on validated PK models for each of these drugs (Sarton *et al.*, 2000; Zoethout *et al.*, 2009; Zoethout *et al.*, 2008). This allowed 1) minimizing the between- and within subject variations in plasma drug concentration and 2) maintaining each of these drugs' concentrations at a plateau level for 90 minutes (approximately 60 minutes after the onset of experiment).

## *Subjects*

Twelve healthy male subjects (age range 18-40; BMI 18-26 kg/m$^2$) were selected to participate in the neuroimaging study. (See supplemental material for exclusion criteria.) The study was approved by the Medical Ethics Review Board of Leiden University Medical Centre. Both oral and written informed consents were obtained from all participating subjects. All studies were performed in compliance with the law on clinical trials of the Netherlands (WMO). Each participant was scanned on three separate days, at least 7 days apart. Subjects fasted for at least four hours prior to the start of a study day. After arrival at the hospital a light standardized meal was provided. On each study day, negative scores on alcohol breath tests and a urinary drug screen for amphetamines, cocaine, morphine and Δ9-Tetrahydrocannabinol (THC) were required. Three intravenous cannulas (one for morphine or placebo administration, one for alcohol or placebo administration and one for blood sampling) were placed in veins of the arms. Before the start of drug or placebo administration, a baseline resting-state scan was made and two baseline measurements of each visual analogue scale (VAS) were taken. After the last scan, the intravenous cannulas were removed and a second meal was provided.

## *Morphine Infusion Protocols*

In order to reach stable serum levels of morphine (approximately 80 nmol/L) an initial bolus of 100 µg/kg/hour was infused during one minute; followed by a continuous infusion of 30 µg/kg/hour for 2.5 hours. Total volume of morphine infusion was approximately 14.5 mg. A prior morphine study using an identical infusion paradigm (Sarton *et al.*, 2000) showed that this infusion regimen could be safely applied, without the occurrence of major side effects. This dose was also associated with significant pharmacodynamic CNS effects. The total amount of morphine administered during one occasion using this dosage scheme, was approximately 14 mg for an average weighted male subject, infused over a time period of 2.5 hours. This is considered to be a safe and rational dose, since it is within the therapeutic range of morphine (i.e. 2.5 mg - 15 mg in 4-5 ml in 4-5 minutes intravenously, for acute pain). To determine the plasma concentration of morphine, venous blood was collected in 5 ml plain tubes (Becton and Dickinson). Blood samples were taken at 0, 15, 30, 50, 60, 90, 120, 150, 180, 210 and 270 minutes after the start of the placebo or drug administration. All samples were centrifuged for 10 minutes at 2000 G between 30 and 45 minutes after collection. Plasma samples were stored at -21° C. Plasma concentrations of morphine were determined using liquid chromatography with tandem mass spectrometry (Sarton *et al.*, 2000).

## *Alcohol Infusion Protocol*

Alcohol concentrations were controlled based on an intravenous alcohol clamping paradigm using ethanol 10% in glucose 5% (O'Connor *et al.*, 1998). We aimed to maintain alcohol levels at 600 mg/L, which barely exceeds the legal limits for driving in the Netherlands (approximately equivalent to two glasses of wine). The alcohol clamp has previously been well-tolerated at this serum level and produced statistically significant pharmacodynamic CNS effects (Zoethout *et al.*, 2009). Infusion rates required to maintain stable alcohol levels were computed by a non-blind staff member without any other involvement in the study, based on measurements of breath alcohol (BrAC) at 5-minute intervals between 0-30 minutes, at 10-minute intervals between minutes 30-60, and 30-minute intervals between minutes 60-300 after the start of the placebo or drug administration. The alcohol placebo condition consisted of a sham-procedure using a glucose 5% solution, including computer-driven adaptations of infusion rates and BrAC measurements.

## *Neuroimaging Acquisition and Processing Protocols*

A 3T Achieva scanner (Philips Medical System, Best, The Netherlands) was used for image acquisition. For each subject we obtained 21 resting-state T2*-weighted acquisitions (gradient echo EPI with parameters set to a TR = 2180 ms, TE = 30 ms, flip angle = 80; 64x64x38 isotropic resolution 3,44 mm, 220 frames, 8 minutes) and a T1-weighted high resolution scan for anatomical registration. During scanning, a pulse oximeter (INVIVO MRI 4500, Siemens Healthcare, Germany) was used to monitor heart rate and oxygen saturation. A flexible pressure belt was used to record the respiratory signals. These RS-FMRI data were preprocessed using the standard procedure including motion correction, brain extraction, Gaussian smoothing with a 5 mm FWHM, kernel, mean-based intensity normalization of all volumes by the same factor (i.e., 4D grand-mean), and high-pass temporal filtering (FWHM = 100 s). After preprocessing, the functional scans were affine-registered to an MNI152 standard space (Montreal Neurological Institute, Montreal, QC, Canada). In all stages Functional Magnetic Resonance Imaging of the Brain (FmriB) Software Library (fsl 4.0, Oxford, UK; www.fmrib.ox.ac.uk/fsl) was used.

## *Assessment of Drug Effects on RSN Connectivity*

We defined RSN connectivity in terms of the similarity of the BOLD fluctuations in each brain voxel in relation to characteristic fluctuation in eight predefined networks of interest (NOI). These networks are obtained from a weighted mask of networks that are most reliably (and reproducibly) identi-

fied from a model-free analysis of the spatio-temporal structure of the resting-state BOLD fluctuations (Beckmann *et al.*, 2005). These template NOIs include over 80% of the total brain volume and comprise: medial and lateral visual systems (NOIs 1 and 2, respectively), auditory and somatosensory system (NOI3), sensory motor system (NOI4), the default mode network (NOI5), executive salience network (NOI6), and visual-spatial and working memory networks (NOIs 7 and 8, which represent almost mirrored networks). Each NOI represents shared neurophysiological fluctuations of the anatomical locations it includes.

To measure connectivity, we used the dual-regression method (Beckmann *et al.*, 2009). Briefly, dual-regression is based on first extracting the temporal pattern of resting-state signal fluctuations within an RSN — for each resting fMRI dataset; and next regressing these 'fitted time courses' against fluctuations in the entire brain. Dual- regression analysis generates statistical maps of z-scores that represent connectivity to the given NOI. In other words, the higher the absolute value of the z-score, the stronger the connectivity to an NOI. These statistical maps can then be used in voxel-wise mixed model analyses of complex experimental designs to obtain a statistical representation of where the drug interactions with any particular network connectivity are significant. The statistical sensitivity of the dual-regression method has been successfully demonstrated in a study that reported distinct differences in brain connectivity in young carriers of the APOE4 gene (Filippini *et al.*, 2009).

Here, dual-regression resulted in 252 statistical parametric maps of whole brain connectivity to each of NOIs (12 subjects x 7 RSfMRIs x 3 treatments x 8NOIs). For each NOI, the respective RSN connectivity maps were entered in a mixed-effect generalized linear model (GLM) to identify which brain regions and which networks were most significantly affected by the drug x time interactions. We used fixed factors treatment and time, and random factor subject. Particularly, we tested the difference between morphine-placebo and alcohol-placebo, while accounting for the variance across time (6 post-injection time points vs. the first pre-infusion). The effects of morphine versus placebo; alcohol versus placebo, each of the time points 2 to 7 versus the pre-drug time point, and an intercept for each subject were modeled as covariates.

Pharmacologically induced variations in heart rate and respiration rate were expected. Previous studies have shown that both heart rate (Chang *et al.*, 2009; Shmueli *et al.*, 2007) and respiration (Birn *et al.*, 2008; Chang and Glover, 2009b; Wise *et al.*, 2004) fluctuations introduce variance in the resting-state BOLD signal. We controlled for global effects of respiration and heart rate by examining the linear association of average heart rate and average respiration rate with resting-state connectivity of each network. We also tested separate models, with and without respiration and heart rates as covariates to examine the robustness of detected effects to nuisance variables.

Permutation-based statistical inference (Nichols and Holmes, 2002) (5000 permutation tests) was used. Statistical significance was set at $p<0.05$, after cluster-based correction for family wise errors (based on the null distribution of the max cluster size across the image) was performed. In all stages FSL 4.0 was used.

## *Pharmacodynamic Assessment*

Computerised Visual Analogue Scales (VAS) were used to measure subjective CNS effects of drugs at baseline and repeated at 30, 60, 90, 120, 150, 180 and 210 minutes after infusion started. The assessments were performed outside the scanner. The VAS Bond and Lader (Bond and Lader, 1974) was used for the subjective assessment of the state of mind at that moment. Three factors corresponding to 'alertness', 'mood' and 'calmness' can be derived from the VAS Bond and Lader. The VAS Bond and Lader scores are expressed in millimeter (mm), in which 50 mm indicates a normal feeling.

An adapted version of the VAS Bowdle (Bowdle *et al.*, 1998) was used for subjective assessment of psychedelic effects. From the VAS Bowdle, three factors corresponding to 'internal perception' and 'external perception' (two modalities of psychedelic effects) and 'feeling high' can be derived. 'External perception' consist of the VAS scores changing of body parts, changes of surrounding, altered passing of time, difficulty controlling thought, changes in

color intensity and changes in sound intensity. It indicates a misperception of an external stimulus or a change in the awareness of the subject's surroundings. 'Internal perception' reflects inner feelings that do not correspond with the reality, e.g. hearing of unrealistic voices or sounds, unrealistic thoughts, paranoid feelings and anxious feelings. 'Feeling high' is a separate item of the VAS Bowdle. The minimum score for the VAS Bowdle (absence of psychedelic effects) is 0 mm. We also used VAS nausea (Mearadji *et al.*, 1998) and VAS alcohol effect (intoxication), each consisting of a single scale in which the extreme left side (0 mm) corresponds to 'not nauseous/drunk at all' and the extreme right side (100 mm) to 'maximum nauseous/drunk'.

Repeatedly measured pharmacodynamic and physiological data were compared with a mixed model analysis of variance with fixed factors treatment, period, time, and treatment by time and random factor subject, subject by treatment and subject by time and the average pre-value (average over all measurements at or before time=0) as covariate (SAS for windows V9.1.2 ; SAS Institute, Inc., Cary, NC, USA). Images were generated using Prism 5, GraphPad Software Inc., La Jolla, CA, USA).

# RESULTS

## *Controlled Pharmacokinetic Profiles*

To reduce inter- and intra-subject variability, we aimed to examine variations in resting-state connectivity under controlled pseudo-steady state plasma drug concentrations, using a target-controlled infusion regimen for morphine and an intravenous clamp for alcohol. Figure 2 illustrates the concentrations over time for each subject. Sixty minutes after the start of the infusion at the onset of RS-FMRI 2, the between-subject averaged (± SD) morphine level was 67.17± 10.22 *(nmol/*L), which remained in the same range in the following RS-FMRIS 3, 4 and 5 (68.63 ± 8.0; 66.88 ± 5.8; 68.04 ± 8.8, respectively). Average alcohol concentrations were also stable, with low between-subject variability at RS-FMRI 2, 3, 4 and 5 (0.60 ± 0.05, 0.60 ± 0.056; 0.58 ± 0.069 and 0.63 ± 0.038 (*g*/L), respectively.)



## *Pharmacodynamic Effects of Morphine and Alcohol*

Figure 3 and table 1 summarize the pharmacodynamic effects. Morphine significantly reduced the respiration and heart rates and increased calmness and sensation of nausea compared to placebo. Alcohol significantly increased the heart rate and feelings of intoxication. Other effects did not reach statistical significance.

## *Effects of Physiological Factors on RSN connectivity*

Figure 4 shows overlaid F-stat maps for each network, at $p < 0.05$ (cluster corrected). Simple regression shows significant correlation between respiration rate and connectivity patterns of NO14, NO15, NO16 and NO17. In contrast, heart rate correlated with connectivity of several areas including the cerebellum, the brainstem and the amygdala in relation to NO13. Overlapping heart rate modulation of connectivity of a region close to major arteries (and extending to the amygdala) in relation to NO1 4, NO15, NO16 and NO18 was also present. However, when effects of treatment by time were modeled in the GLM, the patterns of correlation between physiological factors and connectivity were diminished. Including respiration and heart rate, the topography of morphine effects were changed, but alcohol effects were unchanged (figure 4). With the exception of the default mode network, it seems drug effects on resting-state connectivity were independent of global physiological variations of heart rate and respiratory depression (due to morphine).

## *Interactions of Morphine and Alcohol with RSN Connectivity*

Considering the location of regions where including physiological effects in the statistical model resulted in significant differences (white matter and a zone peripheral to the default mode network in relation to respiration), we expect these effect are non-neuronal and related to global cerebrovascular responses, potentially resulting from a hypercapnic condition due to respiratory

depression (Pattinson *et al.*, 2007), or physiological noise (Birn *et al.*, 2008). Therefore, for the purpose of this study, we have reported drug by time interactions while including these variables in the GLM, to avoid such confounds.

Figure 5 illustrates statistical maps (F-test; cluster p-values <0.05, corrected) of areas where connectivity in relation to a given NOI (in red) was significantly different due to morphine (green) and due to alcohol (blue) over time. Details in terms of cluster size, cluster p-value and the t-value of the peak of the cluster are provided in table 2.

MORPHINE Effects of morphine on RSN connectivity over time (compared to placebo) were significant and dissociable in different NOIs. The affected areas include prefrontal regions (subgenual ACC, medial prefrontal and basolateral prefrontal regions), posterior parietal areas (precuneus, posterior cingulate), medial temporal regions (amygdala and the hippocampal), primary sensory, primary motor, basal ganglia and cerebellum. The most extensive effects of morphine were observed in NOI4 (primary sensory motor network). Within the total areas affected (52.6 ml of brain volume) 39% of the effect was in the bilateral somatosensory areas (inside NOI4), but the rest of the effects were distal to NOI4 (26% in the limbic system and basal ganglia, 16% in the primary motor, 13% in the cerebellum and 10% in the visual area). The next most extensive effects were in the executive salience network, NOI6 (15.13 ml, 73% of which was prefrontal area that lies inside NOI6).

ALCOHOL Compared to morphine, effects of alcohol on RSN connectivity were more limited. The most extensive effects of alcohol were observed in NOI3 (15.15 ml of brain volume), where 62% of the change was in the posterior parietal cortex and the rest in the cerebellum and brainstem (which are outside NOI3). Small changes in connectivity of dorsocaudal ACC and precentral gyrus to NOI4 were present as well (4.52 ml) and in a small area (2.46 ml) inside NOI1.

OVERLAP In NOIs 1, 2, 3, 5, 6, and 7, the intersection of the significant clusters of each drug's effects did not reveal overlap, suggesting topographic differences in each drug effect on these functional networks. Only a small (42 voxels = 0.34 ml) overlap was observed in connectivity of the cerebellum to NOI4 and in connectivity of the superior frontal gyrus to NOI8 (52 voxels = 0.416 ml).

## *Post hoc Examination of Selected ROI Responses*

The purpose of the post-hoc analysis is to demonstrate the range and profile of changes in connectivity in some exemplar ROIs in relation to PK and PD profiles. These ROIs were chosen from NOIs that were most prominently affected by alcohol (NOI3) or morphine (NOI4).

In the sensorimotor network (NOI4), where the negative hippocampal connectivity emerged (figure 6-a), the hippocampal connectivity in relation to NOI4 was small in alcohol and placebo conditions (95% CI: -1.176 to -0.1104 and -1.230 to 0.09146; respectively). By contrast, morphine infusion increased the absolute value of hippocampal connectivity to NOI4 (95% CI: -4.309 to -3.043). We note that connectivity is defined in terms of linear fitting of spontaneous fluctuations at any given region to the 'specific' fluctuations within the entire network (i.e. the weighted average time course of all voxels). Therefore, the negative z-score suggests a distinct inverse relationship in terms of simple oscillations also a phase shift of the fluctuations of the hippocampus with respect to the sensory-motor network. By contrast, the connection of the central gyrus to NOI4, which was similar prior to both infusions, remained stable for alcohol and placebo (95% CI: 8.08 to10.45; and 8.34 to 10.33, respectively) but became stronger after morphine infusion (95% CI: 11.79 to 13.20) (figure 6-b).

Figure 6-c illustrates that alcohol significantly increased the connectivity within NOI1 within the first 90 minutes of infusion (95% CI: 0.36 to 2.22). By contrast, in the brainstem (figure 6-d) morphine and placebo showed an increase in negative connectivity to NOI3 (95% CI: -0.97 to -2.26 and -0.53 to -2.37; respectively), whereas this probably adaptive effect was not present with alcohol (95% CI: -0.07 to 0.87).

## DISCUSSION

Effects of morphine and alcohol on changes in the RSN connectivity were measured at several time points (together with the PD and PK profiles of each drug). We detected effects where the within-subject variation in pre-infusion connectivity in relation to a given NOI was minimal, whereas the difference in RSN connectivity (in relation to placebo) increased over the next six time-points—after plasma concentrations became stable and during the recovery phase. Drugs produced distinct CNS and clinical responses in terms of PD effects, physiological responses, and resting-state connectivity.

The question of the neurological substrates of resting-state BOLD fluctuations is still an open one. The BOLD signal originates from changes in cerebral blood flow, cerebral metabolism and oxygen extraction. At the present state of knowledge, interpretations of BOLD resting-state connectivity are tentative; although evidence for electrical (Britz *et al.*, 2010; Mantini *et al.*, 2007) and arterial perfusion (Chuang *et al.*, 2008) bases of functional connectivity in some of the putative resting-state networks is already available. Notwithstanding a definite biological interpretation of connectivity, we detected effects in most brain regions where changes in receptor binding, cerebral blood flow, or function in response to these specific substances are previously reported. For instance, PET studies with opiodergic radiotracers have shown that the ACC, opercular/insular cortex, thalamus, amygdala and putamen (the medial parts of the pain system) have the highest, and the primary somatosensory, sensorimotor areas (the lateral parts of the pain system) (Baumgartner *et al.*, 2006; Jones *et al.*, 1991; Zubieta *et al.*, 2001) and occipital areas (Sadzot *et al.*, 1991) to have the lowest binding potentials. As table 2 shows, we have detected predominant morphine effects both in areas that, according to PET studies, have low opioid binding potentials (such as primary sensorimotor connectivity to NOI4), and areas that have high opiodergic binding potentials (such as the ACC connectivity to NOI6). This observation precludes interpretation of the effects simply as an outcome of metabolic modulation at the site of receptor action. However, it is possible that the detected effects reflect interactions between these different regions in terms of functional adaptation. Future studies of combined RSfMRI and opiodergic PET studies can shed a light on this central question.

On the other hand, we have been able to demonstrate different connectivity effects resulting from morphine and alcohol, which have different sites of action. Unlike morphine, CNS effects of alcohol are primarily mediated via $GABA_A$ receptors, which are expressed across the brain, although different parts of the brain have higher affinity for different subunits (Kumar *et al.*, 2009). Presently, there are no radiotracer studies to have illustrated alcohol-induced variances in regional $GABA_A$ binding potentials in humans. The most direct *in vivo* evidence for the effect of alcohol on cerebral activation is observed in terms of reduced global metabolism (de Wit *et al.*, 1990; Volkow *et al.*, 2008; Volkow *et al.*, 2006; Wang *et al.*, 2000), with more relative decreases in the occipital cortex (Schreckenberger *et al.*, 2004; Volkow *et al.*, 2008; Wang *et al.*, 2000) and the cerebellum (Volkow *et al.*, 2008; Wang *et al.*, 2000), and relative increases in the brainstem, striatum and the ACC (Schreckenberger *et al.*, 2004). Also, a radiotracer study of a $GABA_A$ ligand ($[^{11}C]$,Ro 15-4513, which has preferred binding potential for ethanol (Hanchar *et al.*, 2006)) in monkeys indicates that the ACC, insula and the limbic system have the highest, and the occipital cortex and the cerebellum have the lowest binding potential for $[^{11}C]$,Ro 15-4513 (Maeda *et al.*, 2003). Here, we observed that alcohol affected the connectivity of the visual cortex (in relation to NOI1), the cerebellum (in relation to NOI3 and NOI4), the ACC (in relation to NOI3 and NOI4) and the brainstem (in relation to NOI3). Surprisingly, the most extensive effect of alcohol was in changing the connectivity of PCC (in relation to NOI3). It is known that alcohol effects can vary with dosage (Blaha *et al.*, 2003; de Wit *et al.*, 1990; Gordon *et al.*, 1995; Luksch *et al.*, 2009; Sano *et al.*, 1993), and they may depend on interindividual differences in regular alcohol consumption. The lesser extent of detected alcohol effects in our study can be hypothetically attributed to these sources of variance and future studies need to address the issue more closely.

With the exception of a small overlap in the cerebellum (in relation to NOI4) and the superior frontal gyrus (in relation to NOI8), drug effects on connectivity were distinct. Similarly, overlap in pharmacodynamic effects was limited. Alcohol significantly increased a feeling of drunkenness and morphine significantly increased nauseous sensation. The CNS effects expected to be common in both drugs such as calmness, alertness and mood were not significant for alcohol (although calmness was significantly increased by morphine). Of course, we cannot conclude that alcohol and morphine do not interact on common brain circuitry. In this experiment, the VAS scores indicate little overlap in terms of subjective changes in mood and feelings induced by alcohol and morphine. However, alcohol (ethanol) was administered at relatively low levels (0.6 g/L), whereas morphine was given in a therapeutically relevant dose (14.5 mg) with considerable functional impact. It is likely that higher doses of alcohol intoxication that result in stronger cognitive and affective responses, will elicit more pronounced changes in local functional connectivity. Presently, without extensive psychometric tests the behavioral correlates of the observed CNS effects cannot be discussed. More precise recordings of certain aspects of emotion and cognition would have enabled us to study the functional significance of RSN connectivity changes. In this experiment, we omitted cognitive testing between different resting-state measurements to avoid introducing performance-related confounds. In fact, our study underlines an important advantage of the resting-state pharma-fMRI (RS-PhfMRI). Significant changes were detected in regions that are expected to be associated with the CNS effects of these drugs; without *a priori* models and performance- or task-related confounds.

It is crucial to note the effects of global physiological variations due to morphine and alcohol. Previous studies have well documented that respiratory depression due to opiodergic drugs generates hypercapnic conditions that increases cerebral blood flow (MacIntosh *et al.*, 2008), and causes focal BOLD signal reduction in response to hypercapnic condition in the sensorimotor brain regions (Pattinson *et al.*, 2007). On the other hand, it has been shown that BOLD fluctuation correlating with respiration and heart rate can compromise delineation of the default mode network (Chang *et al.*, 2009; Chang and Glover, 2009b). Nevertheless, the impact of physiological noise on BOLD is nearly global and including the timecourse of physiological fluctuations do not drastically change the results of connectivity estimation (Birn *et al.*, 2006; Chang and Glover, 2009a). We observed a significant respiratory depression after morphine injection and an increase in heart rate due to alcohol. Our study does not address effect of physiological variables in dual regression outcome, but we have examined the effects of overall physiological variations (in terms of average respiration and average heart rates per each subjects per each session) on resting-state connectivity, and have shown that inclusion of physiological covariates in a repeated measures model does not change the main effects of the drug by time interaction. Interestingly, including respiration and heart rate in the model removes emerging connections from white matter to NOI4, and reduces the extent of morphine effect on connections to the NOI5, the default mode network, whose fluctuations seem to overlap in frequency with spontaneous BOLD changes in the default mode network (Birn *et al.*, 2006; Wise *et al.*, 2004). It should be noted that our framework is based on examining connectivity to eight NOI templates corresponding to the most consistently determined RSNs. These template networks are initially obtained from independent component analyses (CO). It has been suggested that the default-mode network obtained from ICA might not be fully respiration-proof (Birn *et al.*, 2008). It is therefore striking that modeling a global measure of respiration change at the group level analysis would demonstrate an effect expected from more careful analysis of the respiration spectra (Birn *et al.*, 2006; Wise *et al.*, 2004). We cannot preclude the possibility that variation in the temporal physiological profiles have a stronger explanatory power on effects of some of these networks, such as NOI4. Our aim in this study was to show that RS-fMRI is a sensitive and applicable method for detecting drug effects in the brain. Future studies that aim to validate RS-fMRI in relation to specific metabolic effects of especially opiodergic drugs should make precise recordings of variables such as end-tidal $CO_2$ or arterial $CO_2$ tension during the RS-fMRI session and incorporate them in such analyses.

It is worth mentioning that, without considering the time and the session effects in the model, we have detected significant associations between the heart rate and connectivity of several regions outside of NOI3 in relation to this network, in addition to changes in connectivity of a region near major arteries (circle of Willis) that also extends to the amygdala, in relation to NOI3, NOI4, NOI5, NOI6 and NOI8. By contrast, respiration changes affected connectivity to NOI4, NOI5, NOI6 and NOI7. An understanding of the neural or vascular substrates of physiological modulation is potentially crucial to interpretation of the neurological substrate of resting-state BOLD connectivity. Especially in pharmacological studies, the autonomic responses to the CNS drug are central to the research and these questions should be carefully considered in the study design. For instance, heart rate modulated the connectivity of amygdala to NOI4 (sensorimotor), NOI5 (default mode network), NOI6 (salience executive) and NOI8 (right dorsomedial visual stream). This observation is striking, since amygdalar association with visual-emotional (Critchley *et al.*, 2005; van Marle *et al.*, 2009) or executive-motor (Napadow *et al.*, 2008) modulation of the heart rate is previously reported. Regardless of neurobiological interpretations, our findings illustrate that different NOIs vary in degree of susceptibility to physiological modulation; and highlight a need for considering different statistical models to ensure important results are not obscured.

Our study overcomes some limitations in earlier pharmacological fMRI studies, and poses challenging questions. We have successfully detected effects reported in previous studies of morphine and alcohol—without subjectively delineating an ROI necessary for commonly used seed-based RS-fMRI analysis (Anand *et al.*, 2007; Hong *et al.*, 2009; Kelly *et al.*, 2009; Rack-Gomer *et al.*, 2009). It may be argued that predefined NOIs limit the scope of observations by restricting the criterion of connectivity to temporal similarity with a given NOI. However, these networks were chosen on the basis of previous studies that robustly reproduced them in entirely different population (Beckmann *et al.*, 2005; Damoiseaux *et al.*, 2006). By choosing these networks we avoided typical ambiguities associated with ICA approach



that depends on choosing the model order, or on subjective selection of similar or relevant components for further analysis. Nevertheless, we have detected significant changes in connectivity of regions such as the cerebellum and the hippocampus that are outside the reference NOIs. Therefore this method seems to be robust and less limiting than alternative ICA or ROI methods in detecting regions where the drug effects may not be expected. New approaches such as eigenvector centrality mapping (ECM) (Lohmann *et al.*, 2010) might bring us closer to the goal of total model-free analyses, but such methods are computationally more costly than dual-regression using pre-defined NOI templates, as we did. It would be interesting to compare results from ECM analysis and our proposed methodology.

An important advantage of resting-state connectivity, compared to other (more quantitative) neuroimaging methods is that it reveals the complexity of the temporal profile of drug effects in each region or interest. For instance, no significant connection is present between the hippocampus and the sensorimotor network (NOI4) under placebo or alcohol conditions, but during morphine infusion, a significant negative connectivity emerges. At the same time, morphine diminishes the connection of the supplementary motor area to NOI4 to zero. To date, the issue of negative connectivity remains a topic of debate (Murphy *et al.*, 2009). Several hypothetical explanations are possible: It may be argued that global vascular effects of morphine (especially due to respiratory depression) would give rise to the observed negative connectivity demonstrated in the hippocampus. However, these particular emerging negative correlations are anatomically confined to bilateral hippocampus, and although we cannot comment on the neurophysiological basis of the effect, they are unlikely to be non-specific artifacts. Another possibility is that reduction of physiological noise (e.g. due to respiratory depression due to morphine) would enhance negative correlations (Fox *et al.*, 2009). Alternatively, the negative connectivity in the hippocampus may correspond to a delayed, and perhaps adaptive function of this structure (Bast 2007; Khalili-Mahani *et al.*, 2010). We remind that these particular effects were not affected by inclusion of respiration and heart rate averages in the group-

level statistical model. Such inter-regional and inter-network heterogeneity of effects raise questions about compensatory and adaptive mechanisms that interact with the drug (which reflects interactions of different brain regions with each other); and underlines the added advantage of resting-state connectivity analysis compared to other neuroimaging modalities.

In conclusion, we have shown that drug-class specific effects on dynamics of brain function at resting-state can be detected even without *a priori* models. An important advantage of the resting-state Pharma-fMRI is that it is not confounded by differences in alertness or test strategies and other factors that influence the performance and outcomes of task-induced fMRI, and demonstrates effects even if no appropriate task is available. This study was designed to exhibit limited pharmacokinetic variability, and was hence unsuitable to investigate concentration-effect relationships, although the time profiles of the MRI-effects roughly followed those of the clinical responses. This study demonstrates that RS-fMRI could be useful for 'finger-printing' different drug actions within the same individual's brain. Notwithstanding the exploratory nature of the present study, and the inability to characterize the neurophysiological substrates of resting-state BOLD fluctuations, many of our results correspond to findings from previous quantitative PET studies. Because RS-fMRI is noninvasive, widely available and frequently repeatable, it may become an important biomarker for CNS-drug development, able to distinguish detailed drug-induced response patterns in healthy subjects and patients.





Anand A, Li Y, Wang Y, Gardner K, Lowe MJ. (2007). Reciprocal effects of antidepressant treatment on activity and connectivity of the mood regulating circuit: an FMRI study. J Neuropsychiatry Clin Neurosci 19(3):274-82.

Bast T (2007). Toward an integrative perspective on hippocampal function: from the rapid encoding of experience to adaptive behavior. Rev Neurosci 18(3-4):253-81.

Baumgartner U, Buchholz HG, Bellosevich A, Magerl W, Siessmeier T, Rolke R, Hohnemann S, Piel M, Rosch F, Wester HJ, Henriksen G, Stoeter P, Bartenstein P, Treede RD, Schreckenberger M. (2006). High opiate receptor binding potential in the human lateral pain system. Neuroimage 30(3):692-9.

Beckmann C, Mackay C, Filippini N, Smith S. (2009). Group comparison of resting-state FMRI data using multi-subject ICA and dual regression. NeuroImage 47(Supplement 1):1.

Beckmann CF, DeLuca M, Devlin JT, Smith SM. (2005). Investigations into resting-state connectivity using independent component analysis. Philos Trans R Soc Lond B Biol Sci 360(1457):1001-13.

Birn RM, Diamond JB, Smith MA, Bandettini PA. (2006). Separating respiratory-variation-related fluctuations from neuronal-activity-related fluctuations in FMRI. Neuroimage 31(4):1536-48.

Birn RM, Murphy K, Bandettini PA. (2008). The effect of respiration variations on independent component analysis results of resting state functional connectivity. Hum Brain Mapp 29(7):740-50.

Biswal BB, Mennes M, Zuo XN, Gohel S, Kelly C, Smith SM, Beckmann CF, Adelstein JS, Buckner RL, Colcombe S, Dogonowski AM, Ernst M, Fair D, Hampson M, Hoptman MJ, Hyde JS, Kiviniemi VJ, Kotter R, Li SJ, Lin CP, Lowe MJ, Mackay C, Madden DJ, Madsen KH, Margulies DS, Mayberg HS, McMahon K, Monk CS, Mostofsky SH, Nagel BJ, Pekar JJ, Peltier SJ, PETersen SE, Riedl V, Rombouts SA, Rypma B, Schlaggar BL, Schmidt S, Seidler RD, Siegle GJ, Sorg C, Teng GJ, Veijola J, Villringer A, Walter M, Wang L, Weng XC, Whitfield-Gabrieli S, Williamson P, Windischberger C, Zang YF, Zhang HY, Castellanos FX, Milham MP. (2010). Toward discovery science of human brain function. Proc Natl Acad Sci U S A 107(10):4734-9.

Blaha M, Aaslid R, Douville CM, Correra R, Newell DW. (2003). Cerebral blood flow and dynamic cerebral autoregulation during ethanol intoxication and hypercapnia. J Clin Neurosci 10(2):195-8.

Bond A, Lader M. (1974). Use of Analog Scales in Rating Subjective Feelings. British Journal of Medical Psychology 47(Sep):211-218.

Bowdle TA, Radant AD, Cowley DS, Kharasch ED, Strassman RJ, Roy-Byrne PP. (1998). Psychedelic effects of ketamine in healthy volunteers - Relationship to steady-state plasma concentrations. Anesthesiology 88(1):82-88.

Breiter HC, Gollub RL, Weisskoff RM, Kennedy DN, Makris N, Berke JD, Goodman JM, Kantor HL, Gastfriend DR, Riorden JP, Mathew RT, Rosen BR, Hyman SE. (1997). Acute effects of cocaine on human brain activity and emotion. Neuron 19(3):591-611.

Britz J, Van De Ville D, Michel CM. (2010). BOLD correlates of EEG topography reveal rapid resting-state network dynamics. Neuroimage 52(4):1162-70.

Bullmore E, Sporns O. (2009). Complex brain networks: graph theoretical
analysis of structural and functional systems. Nat Rev Neurosci 10(3):186-98.

Chang C, Cunningham JP, Glover GH. (2009). Influence of heart rate on the BOLD signal: the cardiac response function. Neuroimage 44(3):857-69.

Chang C, Glover GH. (2009a). Effects of model-based physiological noise correction on default mode network anti-correlations and correlations. Neuroimage 47(4):1448-59.

Chang C, Glover GH. (2009b). Relationship between respiration, end-tidal CO2, and BOLD signals in resting-state fMRI. Neuroimage 47(4):1381-93.

Chuang KH, van Gelderen P, Merkle H, Bodurka J, Ikonomidou VN, Koretsky AP, Duyn JH, Talagala SL. (2008). Mapping resting-state functional connectivity using perfusion MRI. Neuroimage 40(4):1595-605.

Contet C, Kieffer BL, Befort K. (2004). Mu opioid receptor: a gateway to drug addiction. Curr Opin Neurobiol 14(3):370-8.

Critchley HD, Rotshtein P, Nagai Y, O'Doherty J, Mathias CJ, Dolan RJ. (2005). Activity in the human brain predicting differential heart rate responses to emotional facial expressions. Neuroimage 24(3):751-62.

Damoiseaux JS, Rombouts SA, Barkhof F, Scheltens P, Stam CJ, Smith SM, Beckmann CF. (2006). Consistent resting-state networks across healthy subjects. Proc Natl Acad Sci U S A 103(37):13848-53.

de Wit H, Metz J, Wagner N, Cooper M. (1990). Behavioral and subjective effects of ethanol: relationship to cerebral metabolism using PET. Alcohol Clin Exp Res 14(3):482-9.

Filippini N, MacIntosh BJ, Hough MG, Goodwin GM, Frisoni GB, Smith SM, Matthews PM, Beckmann CF, Mackay CE. (2009). Distinct patterns of brain activity in young carriers of the APOE-epsilon4 allele. Proc Natl Acad Sci U S A 106(17):7209-14.

Fox MD, Snyder AZ, Vincent JL, Raichle ME. (2007). Intrinsic fluctuations within cortical systems account for intertrial variability in human behavior. Neuron 56(1):171-84.

Fox MD, Zhang D, Snyder AZ, Raichle ME. (2009). The global signal and observed anticorrelated resting state brain networks. J Neurophysiol 101(6):3270-83.
Gordon EL, Nguyen TS, Ngai AC, Winn HR. (1995). Differential effects of alcohols on intracerebral arterioles. Ethanol alone causes vasoconstriction. J Cereb Blood Flow Metab 15(3):532-8.
Greicius M. (2008). Resting-state functional connectivity in neuropsychiatric disorders. Curr Opin Neurol 21(4):424-30.
Hanchar HJ, Chutsrinopkun P, Meera P, Supavilai P, Sieghart W, Wallner M, Olsen RW. (2006). Ethanol potently and competitively inhibits binding of the alcohol antagonist Ro15-4513 to alpha4/6beta3delta GABA A receptors. Proc Natl Acad Sci U S A 103(22):8546-51.
Honey G, Bullmore E. (2004). Human pharmacological MRI. Trends Pharmacol Sci 25(7):366-74.
Hong LE, Gu H, Yang Y, Ross TJ, Salmeron BJ, Buchholz B, Thaker GK, Stein EA. (2009). Association of nicotine addiction and nicotine's actions with separate cingulate cortex functional circuits. Arch Gen Psychiatry 66(4):431-41.
Jones AK, Qi LY, Fujirawa T, Luthra SK, Ashburner J, Bloomfield P, Cunningham VJ, Itoh M, Fukuda H, Jones T. (1991). In vivo distribution of opioid receptors in man in relation to the cortical projections of the medial and lateral pain systems measured with positron emission tomography. Neurosci Lett 126(1):25-8.
Kelly C, de Zubicaray G, Di Martino A, Copland DA, Reiss PT, Klein DF, Castellanos FX, Milham MP, McMahon K. (2009). L-dopa modulates functional connectivity in striatal cognitive and motor networks: a double-blind placebo-controlled study. J Neurosci 29(22):7364-78.
Khalili-Mahani N, Dedovic K, Engert V, Pruessner M, Pruessner JC. (2010). Hippocampal activation during a cognitive task is associated with subsequent neuroendocrine and cognitive responses to psychological stress. Hippocampus 20(2):323-34.
Koob GF, Roberts AJ, Schulteis G, Parsons LH, Heyser CJ, Hyytia P, Merlo-Pich E, Weiss F. (1998). Neurocircuitry targets in ethanol reward and dependence. Alcohol Clin Exp Res 22(1):3-9.
Kumar S, Porcu P, Werner DF, Matthews DB, Diaz-Granados JL, Helfand RS, Morrow AL. (2009). The role of GABA(A) receptors in the acute and chronic effects of ethanol: a decade of progress. Psychopharmacology (Berl) 205(4):529-64.
Lohmann G, Margulies DS, Horstmann A, Pleger B, Lepsien J, Goldhahn D, Schloegl H, Stumvoll M, Villringer A, Turner R. (2010). Eigenvector centrality mapping for analyzing connectivity patterns in FMRI data of the human brain. PLoS One 5(4):e10232.
Luksch A, Resch H, Weigert G, Sacu S, Schmetterer L, Garhofer G. (2009). Acute effects of intravenously administered ethanol on retinal vessel diameters and flicker induced vasodilatation in healthy volunteers. Microvasc Res 78(2):224-9.
MacIntosh BJ, Pattinson KT, Gallichan D, Ahmad I, Miller KL, Feinberg DA, Wise RG, Jezzard P. (2008). Measuring the effects of remifentanil on cerebral blood flow and arterial arrival time using 3D GRASE MRI with pulsed arterial spin labelling. J Cereb Blood Flow Metab 28(8):1514-22.
Maeda J, Suhara T, Kawabe K, Okauchi T, Obayashi S, Hojo J, Suzuki K. (2003). Visualization of alpha5 subunit of GABA A/benzodiazepine receptor by 11C Ro15-4513 using positron emission tomography. Synapse 47(3):200-8.
Mantini D, Perrucci MG, Del Gratta C, Romani GL, Corbetta M. (2007). Electrophysiological signatures of resting state networks in the human brain. Proc Natl Acad Sci U S A 104(32):13170-5.
Mearadji B, Straathof JWA, Biemond I, Lamers CBHW, Masclee AAM. (1998). Effects of somatostatin on proximal gastric motor function and visceral perception. Alimentary Pharmacology & Therapeutics 12(11):1163-1169.
Murphy K, Birn RM, Handwerker DA, Jones TB, Bandettini PA. (2009). The impact of global signal regression on resting state correlations: are anti-correlated networks introduced? Neuroimage 44(3):893-905.
Napadow V, Dhond R, Conti G, Makris N, Brown EN, Barbieri R. (2008). Brain correlates of autonomic modulation: combining heart rate variability with fMRI. Neuroimage 42(1):169-77.
Nichols TE, Holmes AP. (2002). Nonparametric permutation tests for functional neuroimaging: a primer with examples. Hum Brain Mapp 15(1):1-25.
O'Connor S, Morzorati S, Christian J, Li TK. (1998). Clamping breath alcohol concentration reduces experimental variance: application to the study of acute tolerance to alcohol and alcohol elimination rate. Alcohol Clin Exp Res 22(1):202-10.
Pattinson KT, Rogers R, Mayhew SD, Tracey I, Wise RG. (2007). Pharmacological FMRI: measuring opioid effects on the BOLD response to hypercapnia. J Cereb Blood Flow Metab 27(2):414-23.
Rack-Gomer AL, Liau J, Liu TT. (2009). Caffeine reduces resting-state BOLD functional connectivity in the motor cortex. Neuroimage 46(1):56-63.
Sadzot B, Price JC, Mayberg HS, Douglass KH, Dannals RF, Lever JR, Ravert HT, Wilson AA, Wagner HN, Jr., Feldman MA, *et al.* (1991). Quantification of human opiate receptor concentration and affinity using high and low specific activity [11C]diprenorphine and positron emission tomography. J Cereb Blood Flow Metab 11(2):204-19.
Sano M, Wendt PE, Wirsen A, Stenberg G, Risberg J, Ingvar DH. (1993). Acute effects of alcohol on regional cerebral blood flow in man. J Stud Alcohol 54(3):369-76.
Sarton E, Olofsen E, Romberg R, den Hartigh J, Kest B, Nieuwenhuijs D, Burm A, Teppema L, Dahan A. (2000). Sex differences in morphine analgesia: an experimental study in healthy volunteers. Anesthesiology 93(5):1245-54; discussion 6A.
Schreckenberger M, Amberg R, Scheurich A, Lochmann M, Tichy W, Klega A, Siessmeier T, Grunder G, Buchholz HG, Landvogt C, Stauss J, Mann K, Bartenstein P, Urban R. (2004). Acute alcohol effects on neuronal and attentional processing: striatal reward system and inhibitory sensory interactions under acute ethanol challenge. Neuropsychopharmacology 29(8):1527-37.
Seeley WW, Menon V, Schatzberg AF, Keller J, Glover GH, Kenna H, Reiss AL, Greicius MD. (2007). Dissociable intrinsic connectivity networks for salience processing and executive control. J Neurosci 27(9):2349-56.
Shmueli K, van Gelderen P, de Zwart JA, Horovitz SG, Fukunaga M, Jansma JM, Duyn JH. (2007). Low-frequency fluctuations in the cardiac rate as a source of variance in the resting-state fMRI BOLD signal. Neuroimage 38(2):306-20.
Smith SM, Fox PT, Miller KL, Glahn DC, Fox PM, Mackay CE, Filippini N, Watkins KE, Toro R, Laird AR, Beckmann CF. (2009). Correspondence of the brain's functional architecture during activation and rest. Proc Natl Acad Sci U S A 106(31):13040-5.
Stein EA, Pankiewicz J, Harsch HH, Cho JK, Fuller SA, Hoffmann RG, Hawkins M, Rao SM, Bandettini PA, Bloom AS. (1998). Nicotine-induced limbic cortical activation in the human brain: a functional MRI study. Am J Psychiatry 155(8):1009-15.
van Marle HJ, Hermans EJ, Qin S, Fernandez G. (2009). From specificity to sensitivity: how acute stress affects amygdala processing of biologically salient stimuli. Biol Psychiatry 66(7):649-55.
Volkow ND, Ma Y, Zhu W, Fowler JS, Li J, Rao M, Mueller K, Pradhan K, Wong C, Wang GJ. (2008). Moderate doses of alcohol disrupt the functional organization of the human brain. Psychiatry Res 162(3):205-13.
Volkow ND, Wang GJ, Franceschi D, Fowler JS, Thanos PP, Maynard L, Gatley SJ, Wong C, Veech RL, Kunos G, Kai Li T. (2006). Low doses of alcohol substantially decrease glucose metabolism in the human brain. Neuroimage 29(1):295-301.
Wagner KJ, Willoch F, Kochs EF, Siessmeier T, Tolle TR, Schwaiger M, Bartenstein P. (2001). Dose-dependent regional cerebral blood flow changes during remifentanil infusion in humans: a positron emission tomography study. Anesthesiology 94(5):732-9.
Wang GJ, Volkow ND, Franceschi D, Fowler JS, Thanos PK, Scherbaum N, Pappas N, Wong CT, Hitzemann RJ, Felder CA. (2000). Regional brain metabolism during alcohol intoxication. Alcohol Clin Exp Res 24(6):822-9.
Wise RG, Ide K, Poulin MJ, Tracey I. (2004). Resting fluctuations in arterial carbon dioxide induce significant low frequency variations in BOLD signal. Neuroimage 21(4):1652-64.
Zoethout RW, Schoemaker RC, Zuurman L, van Pelt H, Dahan A, Cohen AF, van Gerven JM. (2009). Central nervous system effects of alcohol at a pseudo-steady-state concentration using alcohol clamping in healthy volunteers. Br J Clin Pharmacol 68(4):524-34.
Zoethout RW, van Gerven JM, Dumont GJ, Paltansing S, van Burgel ND, van der Linden M, Dahan A, Cohen AF, Schoemaker RC. (2008). A comparative study of two methods for attaining constant alcohol levels. Br J Clin Pharmacol 66(5):674-81.
Zubieta JK, Smith YR, Bueller JA, Xu Y, Kilbourn MR, Jewett DM, Meyer CR, Koeppe RA, Stohler CS. (2001). Regional mu opioid receptor regulation of sensory and affective dimensions of pain. Science 293(5528):311-5.
Zuo XN, Kelly C, Adelstein JS, Klein DF, Castellanos FX, Milham MP. (2009). Reliable intrinsic connectivity networks: Test-retest evaluation using ICA and dual regression approach. Neuroimage. 49:2163–2177.

**FIGURE 1** SCHEMATIC PRESENTATION OF STUDY DESIGN AND DATA COLLECTION *(full colour version inside cover)*

*Each subjects participated in three randomized sessions. Both examiners and the subject were blind to which drug they received. The expected pharmacokinetic profiles for alcohol and morphine are plotted (1). The placebo infusion was conducted concurrently with the drug infusion. After preprocessing (2) dual regression on all data sets to estimate whole-brain connectivity in relation to the eight template RSNs (3), followed by statistical testing (4).*

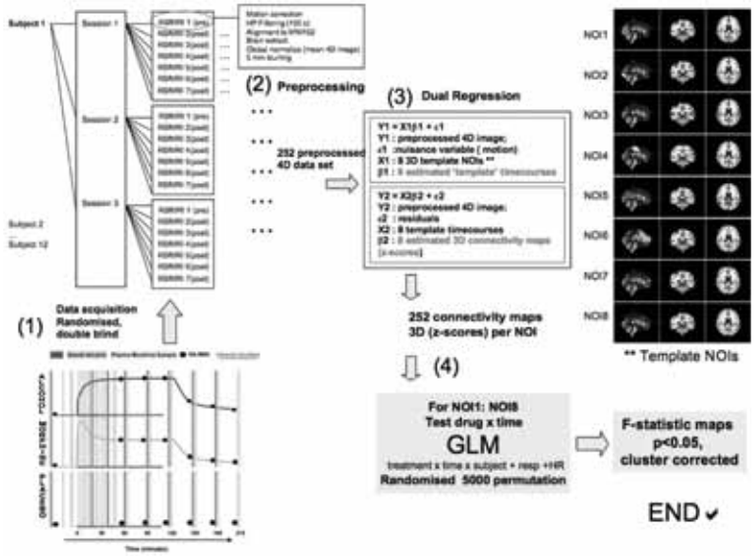


**FIGURE 2** PHARMACOKINETIC EFFECTS

*(a) Plasma morphine concentrations for each subject; (b) Breath alcohol readouts. The bars illustrate when the RS-fMRI acquisition took place.*

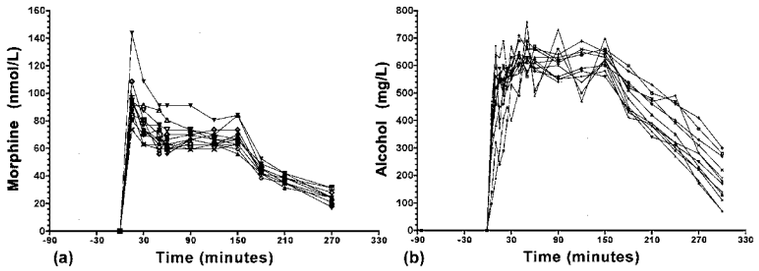


**FIGURE 3** PHARMACODYNAMIC EFFECTS OVER TIME (MEAN ± SEM)

*See table 1 for details of main effects.*

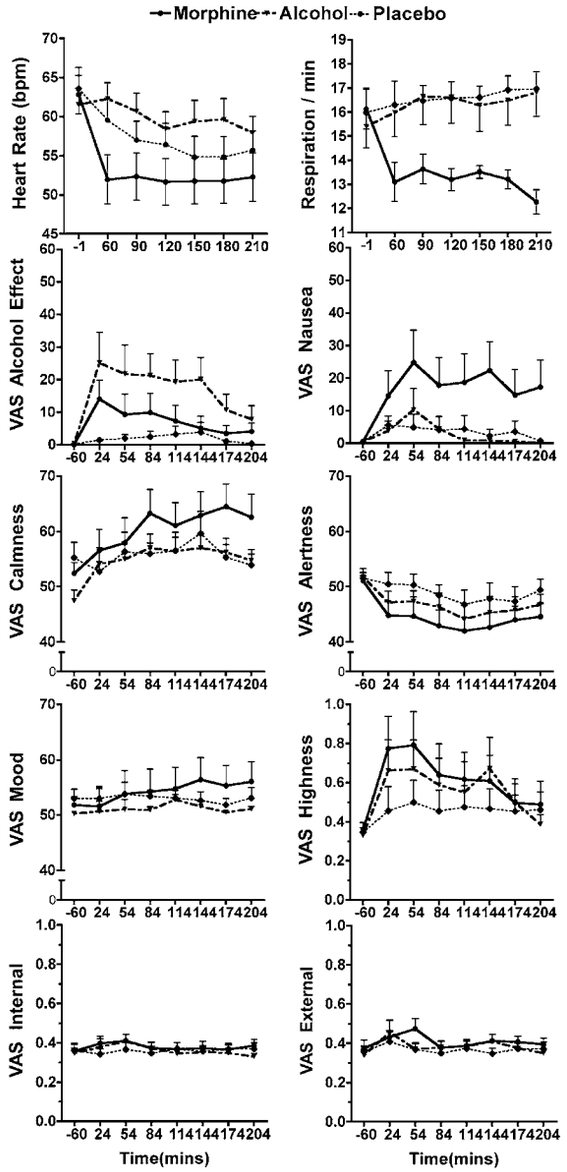

**FIGURE 4** OVERLAYING MAPS OF VOXEL-WISE REGRESSION OF RESPIRATION (RESP) AND HEART RATE (HR) WITH CONNECTIVITY TO THE 8 TEMPLATE NETWORKS *(full colour version inside cover) F-statistics; cluster corrected p<0.05 in GLM, including treatment by time interactions.*

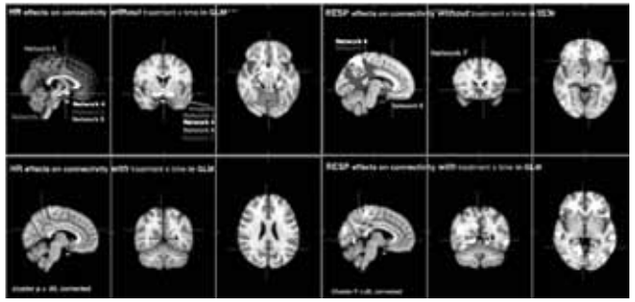

**FIGURE 5** OVERLAYING MAPS OF DRUG BY TIME INTERACTIONS WITH CONNECTIVITY TO THE 8 TEMPLATE NETWORKS *(full colour version inside cover) F-statistics voxel-wise p < 0.0001; cluster corrected p<0.05; average physiological rates included as covariates. The NOIs are represented in pale red, morphine effects in green and alcohol effects in blue. table 2 for the effects details. WM, working memory; DVS, dorsal visual stream.*

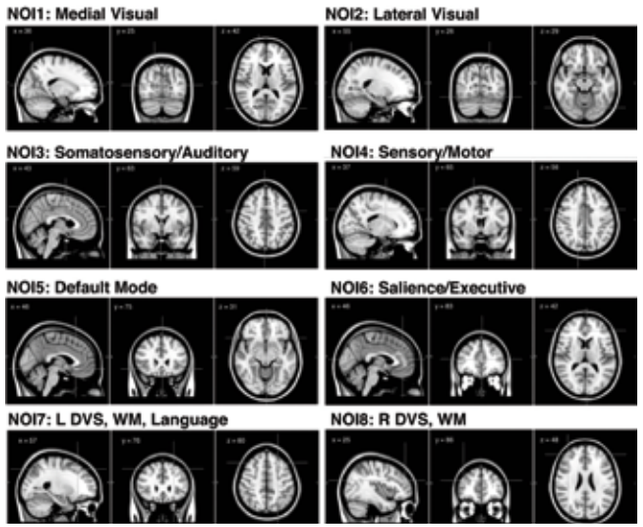




**FIGURE 6** PROFILE OF CHANGE IN RESTING-STATE CONNECTIVITY IN SELECT ROI'S *(full colour version inside cover)*
*Statistical parametric maps (t-statistics, cluster corrected p<0.05) reflect the amplitude of drug-induced changes in functional connectivity (drug versus placebo over time). Morphine leads to increased negative connectivity of the hippocampus (a), and positive connectivity of the central gyri (b) in relation to the sensory-motor network (NOI4). Alcohol enhances the intra-connectivity of the visual network (c) and disrupts adaptive connectivity of brainstem (d). In the ROI diagrams, red corresponds to placebo, green to morphine and blue to alcohol.*

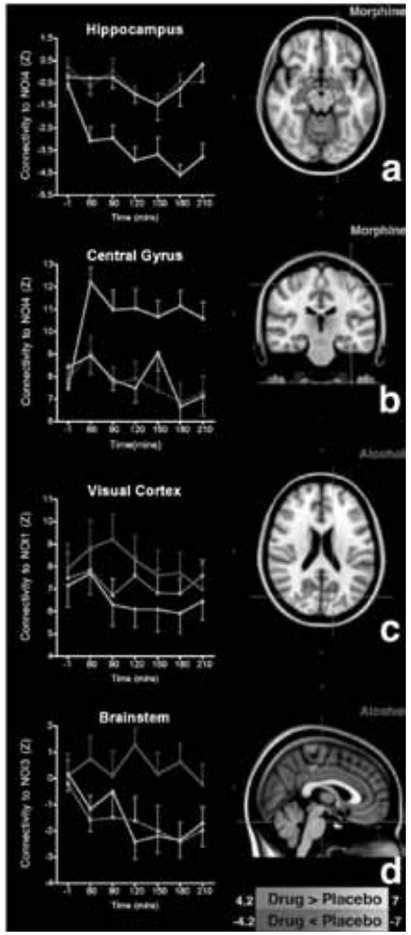

**TABLE 1** PHARMACODYNAMIC EFFECTS

| Pharmacodynamic Effects | | | | | | | |
|---|---|---|---|---|---|---|---|
| | Least Square Means | | | | Contrasts | | |
| Parameter | Placebo | Alcohol | Morphine | Treatment P-value | Alcohol vs Placebo | Morphine vs Placebo | Morphine vs Alcohol |
| VAS Alcohol effects (mm) | 1.7 | 19.1 | 7.2 | 0.0096 | 17.4 (6.7, 28.2) p=0.0030 | 5.5 (-5.1, 16.2) p=0.2907 | -11.9 (-22.7, -1.1) p=0.0321 |
| VAS Alertness (mm) | 48.6 | 46.0 | 43.7 | 0.1843 | -2.6 (-8.0, 2.8) p=0.3236 | -5.0 (-10.3, 0.4) p=0.0696 | -2.3 (-7.7, 3.0) p=0.3742 |
| VAS Calmness (mm) | 53.4 | 58.2 | 60.6 | 0.0428 | 4.7 (-1.5, 11.0) p=0.1323 | 7.2 (1.6, 12.7) p=0.0136 | 2.5 (-3.3, 8.2) p=0.3855 |
| VAS Mood (mm) | 51.7 | 52.8 | 54.4 | 0.5171 | 1.1 (-4.1, 6.2) p=0.6623 | 2.8 (-2.2, 7.8) p=0.2618 | 1.7 (-3.4, 6.7) p=0.4982 |
| VAS Nausea (mm) | 3.7 | 3.0 | 18.6 | 0.0320 | -0.6 (-13.5, 12.2) p=0.9179 | 14.9 (2.1, 27.8) p=0.0247 | 15.6 (2.8, 28.4) p=0.0198 |
| VAS External log(mm) | 0.371 | 0.398 | 0.406 | 0.4601 | 0.027 (-.035, 0.089) p=0.3650 | 0.035 (-.026, 0.097) p=0.2413 | 0.008 (-.054, 0.071) p=0.7826 |
| VAS Internal log(mm) | 0.359 | 0.366 | 0.382 | 0.4592 | 0.007 (-.033, 0.046) p=0.7245 | 0.023 (-.017, 0.062) p=0.2359 | 0.016 (-.024, 0.056) p=0.3934 |
| VAS feeling high log(mm) | 0.467 | 0.575 | 0.635 | 0.5275 | 0.107 (-.202, 0.417) p=0.4766 | 0.168 (-.141, 0.476) p=0.2706 | 0.060 (-.251, 0.371) p=0.6908 |
| Heart Rate | 55 | 61 | 52 | 0.0004 | 5.2 (1.4, 9.0) p=0.0098 | -3.8 (-7.5, 0) p=0.0498 | -9.0 (-12.7, -5.2) p<0.0001 |
| Respiration | 16.6 | 16.6 | 13 | <0.0001 | 0.0 (-1.4 1.4) p = 0.9659 | -3.6 (-5, -2.2) p < 0.0001 | -3.6 (-5, -2.2) p<0.0001 |



**TABLE 2** DETAILS OF DRUG EFFECTS ON FUNCTIONAL CONNECTIVITY

*(cluster corrected threshold, p <0.05)*

| Network | Morphine | | | | | | Ethanol | | | | | |
|---|---|---|---|---|---|---|---|---|---|---|---|---|
| | Location | #voxels | t | x | y | z | Location | #voxels | t | x | y | z |
| **NO11: Medial Visual Network** relaying visual input through thalamus to primary visual area. Includes, Calcarine, inferior precuneus, and primary visual cortex. | R cerebellum | 149 *** | 4.77 | 27 | 28 | 16 | R visual | 140 *** | 4.78 | 35 | 27 | 41 |
| | L cerebellum | 101 ** | 4.8 | 64 | 30 | 15 | L visual | 100 ** | 5.57 | 52 | 26 | 46 |
| | R hippocampus | 65 ** | 5.05 | 33 | 50 | 29 | L parietal lobule | 67 ** | -4.91 | 59 | 31 | 56 |
| | R superior frontal | 87 ** | 5.87 | 37 | 88 | 50 | | | | | | |
| | Precentral gyrus | 26* | 4.88 | 44 | 53 | 71 | | | | | | |
| **NO12: Lateral visual Network** visual spatial attention. | R occipital V5 | 91 ** | 5.52 | 23 | 26 | 40 | R cuneus | 56 ** | 4.9 | 22 | 33 | 21 |
| | L occipital V4 | 70 ** | 4.87 | 57 | 20 | 29 | Precuneus | 24* | 4.45 | 46 | 32 | 43 |
| | L posterior insula | 45* | -5.24 | 65 | 51 | 45 | | | | | | |
| | R superior frontal | 33* | -4.83 | 38 | 88 | 51 | | | | | | |
| **NO13: Superior Temporal Network** auditory, somatosensory and autonomic functions includes insular and dorsocaudal anterior cingualte cortices. | L precuneus | 348 *** | -5.78 | 45 | 29 | 53 | Bi posterior cingulated | 728 *** | 5.3 | 45 | 50 | 59 |
| | R paracingulate | 322 *** | -4.96 | 44 | 67 | 60 | R superior parietal lobule | 310 *** | 5.86 | 27 | 39 | 58 |
| | R cerebellum | 96 ** | -4.57 | 39 | 45 | 26 | Left cerebellum | 167 *** | 4.97 | 49 | 42 | 25 |
| | L cerebellum (tonsil) | 87 ** | -5.31 | 54 | 42 | 13 | Bi culmen | 153 *** | 5.73 | 45 | 37 | 15 |
| | L cerebellum (culmen) | 74 ** | -4.59 | 50 | 44 | 25 | Right cerebellum | 144 *** | 5.03 | 41 | 42 | 25 |
| | L amygdala | 63 ** | -4.6 | 54 | 62 | 25 | brainstem | 144 ** | 6.29 | 43 | 54 | 23 |
| | R amygdala | 40* | -4.28 | 35 | 64 | 25 | L supramarginal gyrus | 109 ** | 5.61 | 68 | 45 | 59 |
| | L frontal pole | 46* | -4.75 | 57 | 86 | 52 | L precuneus | 45* | 4.92 | 47 | 35 | 41 |
| | L occipital superior | 38* | -4.77 | 56 | 26 | 62 | R supramarginal gyrus | 38* | 5.44 | 18 | 45 | 59 |
| | R occipital superior | 44* | -4.37 | 37 | 26 | 58 | L orbitofrontal | 34* | 5.16 | 70 | 76 | 32 |
| | R postcentral | 53* | -4.58 | 18 | 59 | 57 | R anterior cingulate | 22* | 4.80 | 39 | 86 | 36 |

| | | | | | | | | | | | | |
|---|---|---|---|---|---|---|---|---|---|---|---|---|
| **N014: Sensory Motor Network** includes pre- and postcentral somatosensory somatomotor areas | L primary somatosensory cortex | 1774 *** | 7.52 | 65 | 51 | 65 | R cerebellum & fusiform | 223 *** | -5.74 | 27 | 40 | 23 |
| | L hippocampus | 1679*** | -7.61 | 55 | 54 | 29 | L dorsocaudal anterior cingulate | 132 ** | -4.02 | 39 | 61 | 59 |
| | R hipocampus | | -6.06 | 32 | 56 | 29 | R inferior parietal lobule | 112 ** | -4.79 | 19 | 47 | 49 |
| | L putamen | | -4.3 | 58 | 58 | 41 | R precentral R | 98** | -5.3 | 49 | 65 | 56 |
| | L amygdala | | -6.27 | 37 | 61 | 27 | | | | | | |
| | R amygdala | | -6.02 | 52 | 61 | 28 | | | | | | |
| | L caudate | | -4.9 | 52 | 64 | 47 | | | | | | |
| | Bi primary motor | 1001 | 7.18 | 45 | 52 | 66 | | | | | | |
| | L cerebellum VI | **851** | -7.95 | 52 | 30 | 27 | | | | | | |
| | Vermis | | -5.37 | 45 | 29 | 28 | | | | | | |
| | L cerebellum VI | | -5.3 | 39 | 30 | 28 | | | | | | |
| | R primary somatosensory | 722 | 5.7 | 25 | 51 | 62 | | | | | | |
| | R putamen | **668** | -6.28 | 32 | 58 | 41 | | | | | | |
| | R caudate | | -5.53 | 39 | 64 | 46 | | | | | | |
| | L occipital fusiform | 494 | 6.11 | 54 | 19 | 31 | | | | | | |
| | R occipital fusiform | 314 | 6.01 | 33 | 23 | 30 | | | | | | |
| | L posterior insula | 122 | 5.39 | 63 | 52 | 45 | | | | | | |
| | R posterior insula | 84 | 5.12 | 23 | 56 | 44 | | | | | | |
| | thalamus | 87 | -4.64 | 45 | 52 | 41 | | | | | | |
| | Brainstem | 95 | 5.25 | 49 | 47 | 16 | | | | | | |
| | Paracingulate gyrus | 61 | 5.53 | 47 | 80 | 50 | | | | | | |
| **N015: Default Mode Network** Includes rostral medial prefrontal and posterior medial parietal precuneal and PCC areas | L subgen ACC | 40* | -5.27 | 47 | 76 | 31 | | | | | | |
| | L middle front | 40* | -4.81 | 61 | 76 | 59 | | | | | | |
| | Posterior cingulated | 37* | -4.53 | 45 | 40 | 48 | | | | | | |



| | | | | | | | | | | | | |
|---|---|---|---|---|---|---|---|---|---|---|---|---|
| **N016: Prefrontal Network** Includes medial and inferior prefrontal cortices. Regions in this network are implicated in executive control, attention and pain. Includes medial and inferior prefrontal cortices. Regions in this network are implicated in executive control, attention and pain. | Anterior cingulate | 490 *** | -6.47 | 45 | 85 | 41 | | | | | | |
| | L frontal pole | 392*** | -6.31 | 61 | 94 | 36 | | | | | | |
| | R frontal pole | 350*** | -6.65 | 30 | 89 | 50 | | | | | | |
| | R primary motor | 212 *** | -5.7 | 39 | 49 | 69 | | | | | | |
| | L insula | 115 ** | -6.13 | 63 | 71 | 33 | | | | | | |
| | Bi thalamus | 101** | -5.42 | 45 | 62 | 42 | | | | | | |
| | R lingual | 63** | -5.32 | 46 | 18 | 32 | | | | | | |
| | R inferior parietal lob | 50* | -4.82 | 21 | 39 | 51 | | | | | | |
| | L orbitofrontal | 42* | -5.43 | 54 | 71 | 27 | | | | | | |
| | L primary motor | 40* | -5.49 | 50 | 49 | 70 | | | | | | |
| | L lingual | 36* | -4.99 | 52 | 30 | 36 | | | | | | |
| **N017: Left Dorsal Visual Stream Network** Includes Broca rea 44, frontal pole, dorsolateral prefrontal cortex and parietal lobule. Working memory, visual spatial processing and language | L superior frontal | 31* | 4.83 | 46 | 91 | 45 | | | | | | |
| | R frontal pole | 81** | -5.56 | 25 | 86 | 48 | | | | | | |
| | R middle frontal | 55** | -4.8 | 32 | 73 | 63 | | | | | | |
| **N018: Right Dorsal Visual Stream Network** Includes homologous regions as N017, plus right paracingulate gyrus, left posterior cingulated and left medial prefrontal cortex. | L superior frontal | 270 *** | -5.16 | 56 | 75 | 58 | L superior frontal | 79 ** | -5.64 | 55 | 74 | 59 |
| | L basolateral PFC | 243 *** | -5.22 | 67 | 84 | 34 | | | | | | |
| | L superior parietal lobule | 160 *** | -5.36 | 62 | 35 | 60 | | | | | | |
| | Paracingulate, medial prefrontal | 144 *** | -5.29 | 47 | 80 | 56 | | | | | | |
| | R primary somatosensory | 63 ** | -4.83 | 21 | 46 | 63 | | | | | | |
| | L sup middle frontal | 52 ** | -5.5 | 28 | 67 | 63 | | | | | | |
| | R thalamus | 35* | -4.71 | 40 | 53 | 42 | | | | | | |

Cluster significance: * p < 0.05; ** p<0.01; *** p<0.001
Voxel dimension is 2mm x 2mm x 2mm (voxel volume 0.008ml)